# Effect of Solution Viscosity on Intramolecular Electron Transfer in Sulfite Oxidase†

Changjian Feng,‡ Rohit V. Kedia,§ James T. Hazzard,§ John K. Hurley,§ Gordon Tollin,*,§ and John H. Enemark*,‡

*Department of Chemistry, The University of Arizona, Tucson, Arizona 85721, and Department of Biochemistry and Molecular Biophysics, The University of Arizona, Tucson, Arizona 85721*

*Received December 18, 2001; Revised Manuscript Received February 27, 2002*

ABSTRACT: Our previous studies have shown that the rate constant for intramolecular electron transfer (IET) between the heme and molybdenum centers of chicken liver sulfite oxidase varies from ∼20 to 1400 $s^{-1}$ depending upon reaction conditions [Pacheco, A., Hazzard, J. T., Tollin, G., and Enemark, J. H. (1999) *J. Biol. Inorg. Chem. 4*, 390−401]. These two centers are linked by a flexible polypeptide loop, suggesting that conformational changes, which alter the Mo−Fe distance, may play an important role in the observed IET rates. In this study, we have investigated IET in sulfite oxidase using laser flash photolysis as a function of solution viscosity. The solution viscosity was varied over the range of 1.0−2.0 cP by addition of either polyethylene glycol 400 or sucrose. In the presence of either viscosogen, an appreciable decrease in the IET rate constant value is observed with an increase in the solvent viscosity. The IET rate constant exhibits a linear dependence on the negative 0.7th power of the viscosity. Steady-state kinetics and EPR experiments are consistent with the interpretation that viscosity, and not other properties of the added viscosogens, is responsible for the dependence of IET rates on the solvent composition. The results are consistent with the role of conformational changes on IET in sulfite oxidase, which helps to clarify the inconsistency between the large rate constant for IET between the Mo and Fe centers and the long distance (∼32 Å) between these two metal centers observed in the crystal structure [Kisker, C., Schindelin, H., Pacheco, A., Wehbi, W., Garnett, R. M., Rajagopalan, K. V., Enemark, J. H., and Rees, D. C. (1997) *Cell 91*, 973−983].

Sulfite oxidase (SO)[1] catalyzes the oxidation of sulfite to sulfate, coupled with the subsequent reduction of 2 equiv of ferricytochrome *c* [$(\text{cyt } c)_{ox}$] to ferrocytochrome *c* [$(\text{cyt } c)_{red}$] (*1*):

$$SO_3^{2-} + H_2O + 2(\text{cyt } c)_{ox} \rightleftharpoons SO_4^{2-} + 2(\text{cyt } c)_{red} + 2H^+$$

This is the terminal reaction in the oxidative degradation of sulfur-containing compounds, and is physiologically essential. In animals, the enzyme is located in the mitochondrial intermembrane space (*2*, *3*); the most extensively studied examples of SO are from the livers of rats, humans, and chickens, and all of these show a very high degree of amino acid sequence homology (*4*−*6*). Chicken liver SO is typical of the enzyme in higher vertebrates, and consists of two identical subunits, each with a molecular mass of ∼51.5 kDa (*7*). Each subunit has two functionally distinct domains. The smaller N-terminal domain (∼10 kDa) is typical of a small $b_5$-type cytochrome, containing a noncovalently bound heme cofactor; in the resting enzyme, the heme iron is in the oxidation state of $Fe^{III}$. The larger C-terminal domain (∼42 kDa) contains the Mo−pterin cofactor, and the Mo is in the resting oxidation state of $Mo^{VI}$.

Figure 1 summarizes the oxidation-state changes that are thought to occur at the Mo and Fe centers during the catalytic cycle (*8*). The cycle begins with the two-electron oxidation of $SO_3^{2-}$ by $Mo^{VI}$, which cannot be detected by spectroscopy. The first species that is spectroscopically detected is $Fe^{II}$-$Mo^{V}$, probably generated by direct intramolecular electron transfer (IET) from the molybdenum to the iron center. Reoxidation of the $Fe^{II}$ center occurs by one-electron transfer to cytochrome *c*, leaving the enzyme as $Fe^{III}Mo^{V}$. A second Mo to Fe IET step (giving $Fe^{II}Mo^{VI}$), followed by reduction of a second equivalent of cytochrome *c*, returns the enzyme to the resting state ($Fe^{III}Mo^{VI}$). Note that an equilibrium between $Fe^{II}Mo^{VI}$ and $Fe^{III}Mo^{V}$ is established by the second IET step, with rate constants $k_f$ and $k_r$ for the forward and reverse reactions, respectively. These rate constants have been found to be affected by various parameters such as pH, anion concentration, and even the nature of the anion; thus, $Cl^-$, $SO_4^{2-}$, and $PO_4^{3-}$ all have different inhibitory effects (*7*, *9*).

In this study, as well as in the previous reports, we have used the flash photolysis technique to generate the $Fe^{II}Mo^{VI}$ form of SO and to measure $k_f$ and $k_r$ under various conditions, as shown in Figure 1 (*7*, *9*). Using this technique, one directly obtains values for the intramolecular electron transfer rate

† This research was supported by NIH Grant GM37773 to J.H.E., NIH Grant DK15057 to G.T., and Beckman Research Foundation (R.V.K.).

* To whom correspondence should be addressed. J.H.E.: e-mail, jenemark@u.arizona.edu; phone, (520) 626-8065; fax, (520) 626-8065. G.T.: e-mail, gtollin@u.arizona.edu; fax, (520) 621-9288.

‡ Department of Chemistry.

§ Department of Biochemistry and Molecular Biophysics.

[1] Abbreviations: SO, sulfite oxidase; $(\text{cyt } c)_{ox}$ and $(\text{cyt } c)_{red}$, ferricytochrome *c* and ferrocytochrome *c*, respectively; dRF and dRFH•, 5-deazariboflavin and 5-deazariboflavin semiquinone, respectively; EDTA, ethylenediaminetetraacetic acid; PEG 400, polyethylene glycol 400; IET, intramolecular electron transfer; ET, electron transfer; $k_{et}$, rate constant for intramolecular electron transfer; $\eta$, absolute viscosity.

10.1021/bi016059f CCC: $22.00 
Published on Web 04/16/2002

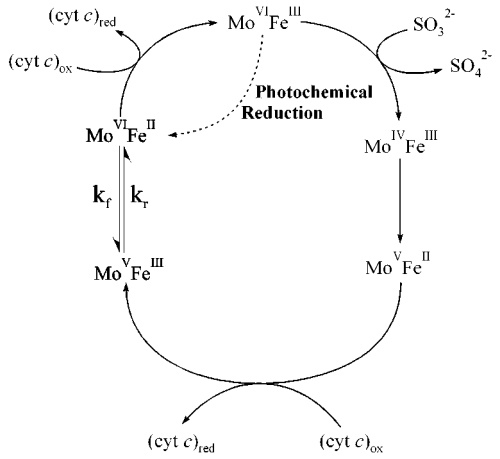


FIGURE 1: Oxidation-state changes at the Mo and Fe centers of SO during the catalytic oxidation of sulfite, and concomitant reduction of cyt *c*. Flash photolysis provides a way to reduce SO by one electron (shown by a dashed arrow connecting $Mo^{VI}Fe^{III}$ to $Mo^{VI}Fe^{II}$) in a solution containing 5-deazariboflavin (dRF) and the sacrificial electron donor semicarbazide. The ensuing equilibrium can thus be observed without creating the intermediate species in the cycle. The rate constants $k_f$ and $k_r$ are defined in the text.

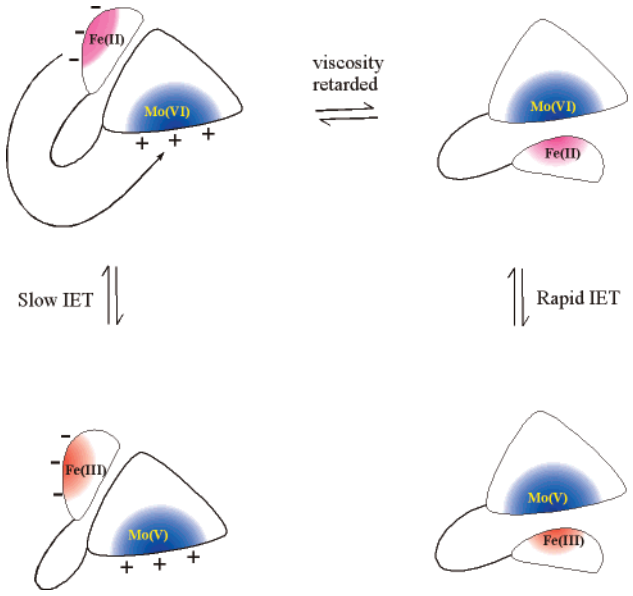


FIGURE 2: Proposed conformational change in sulfite oxidase that could move the Mo and Fe centers closer together than in the crystal structure. Only one subunit of SO is portrayed for clarity.

$k_{et}$ ($=k_f + k_r$) (see below) and the equilibrium constant $K_{eq}$ ($=k_f/k_r$) as described previously (*9*).

Under optimal conditions, the value of $k_{et}$ has been measured to be 1400 $s^{-1}$ (*7*). In the X-ray crystal structure of SO, the Mo and Fe centers are ~32 Å apart (*10*). On the basis of current models for IET over such a large distance, the rate constant should be much less than this ($\leq$100 $s^{-1}$) (*11*, *12*). This indicates that the position and orientation of the redox partners with respect to each other observed in the crystal structure are less than optimal for electron transfer (*9*). One possible explanation for this discrepancy is that the protein conformation during electron transfer in solution is different from that seen in the crystal structure. Rearrangement to a more "productive" orientation may occur before electron transfer, which suggests that fast electron transfer between Mo(VI) and Fe(II) centers requires subtle and precise positioning, orientation, and docking of the two redox partners with respect to each other. Figure 2 shows a schematic drawing of the relative positions of the Mo and Fe domains in the crystal structure, and depicts how the backbone rearrangement of the protein might bring the two redox-active centers sufficiently close together to permit rapid electron transfer between them. The Mo−pterin and heme domains of SO are linked by a very flexible loop consisting of 10 amino acid residues (*10*), which could provide the heme domain with the necessary mobility to allow its negatively charged exposed edge to interact electrostatically with the positively charged Mo site. Indeed, in the crystal structure, the two heme domains do not occupy identical positions in the dimer, suggesting that they may be quite mobile. The existence of such an interdomain flexible loop makes SO a unique candidate for studying the role of protein rearrangement in electron transfer in biological macromolecules.

It is generally accepted that the structural dynamics of proteins in solution plays an important role in regulating their biochemical function (*13*, *14*). The interaction of the protein structure with the surrounding water is well-known to be intimately linked with this type of structural dynamics, and Brownian theory indicates that the internal friction associated with such molecular motion, which is linked to the solvent viscosity, should affect protein dynamics. The role of solvent viscosity in controlling chemical kinetics was proposed by Kramers in 1940 (*15*), and many subsequent experiments have focused on the role of solvent in the dynamics of simple chemical processes, such as intramolecular electron transfer (*16*) and isomerization of substituted azobenzenes (*17*). Due to the complexity of biological reactions, it was not until the end of the 1970s that the applicability of Kramers' theory to protein reactions was demonstrated by Gavish (*18*, *19*). Since then, a large number of studies of solvent viscosity effects on biochemical kinetic processes have been carried out, and in most cases, the observed rate constant $k_{obs}$ has been shown to be inversely proportional to the fractional power ($\alpha$) of the viscosity $\eta$ (eq 1) (*20*, *21*)

$$k_{obs} \propto \eta^{-\alpha} \quad (0 < \alpha \leq 1) \qquad (1)$$

The value of the power dependence $\alpha$ (normally but not always $\leq$1) depends on the nature of the movement (*22*, *23*). Conformational changes that involve major surface changes tend to show pronounced viscosity dependence, for example, the folding rate of DNA coils (*24*) and the loop closure of a DNA hairpin (*25*). Some typical protein-based examples include the catalytic mechanism of enzymes (*26*−*29*), binding of $O_2$ or CO to respiratory proteins (*30*, *31*), and protein conformational changes (*32*), protein dynamics (*33*, *34*), and protein folding (*35*).

Davidson has proposed three types of electron transfer mechanisms between proteins (*36*). One is "true" electron transfer (ET). When the ET step is combined with a fast interconversion equilibrium in the protein complex, the overall reaction is termed "coupled". When the ET step is combined with a slower and thus rate-limiting structural rearrangement, the overall reaction is termed "gated" (*36*, *37*). In the cases of true and coupled ET, the observed ET rates are expected to be independent of viscosity (*38*). Viscosity effects on electron transfer in protein−protein complexes have been extensively studied and used as

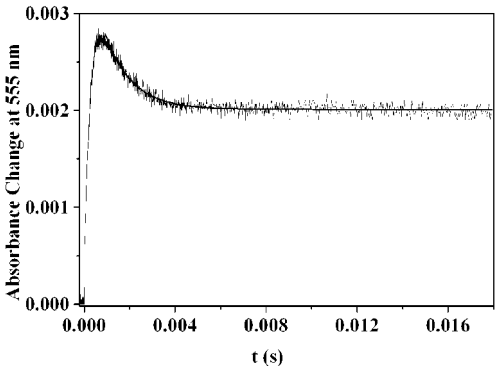


FIGURE 3: Transient kinetic trace obtained at 555 nm upon photoexcitation of a solution containing 24.0 $\mu$M chicken SO, ~90 $\mu$M dRF, 5% (v/v) PEG 400, and 0.5 mM semicarbazide in 10 mM Tris buffer (pH 7.4). The solid line represents a single-exponential fit to the IET phase.

evidence for electron transfer gated by dynamic fluctuations in the interprotein orientation in the bound complex (*39*−*42*). An example of this is provided by a recent study on the viscosity dependence of the cytochrome redox reaction in the cytochrome $b_6f$ complex, which implies the motion of the Rieske iron−sulfur protein during electron transfer (*43*). To the best of our knowledge, very few studies of the effect of viscosity on *intramolecular* electron transfer in proteins have been reported. To determine if changes in the SO conformation have an effect on IET, herein we have measured the effect of solution viscosity on the IET rate constant ($k_{et}$) using the laser flash photolysis technique.

## EXPERIMENTAL PROCEDURES

*Materials.* PEG 400 and sucrose were obtained from Sigma Chemical Co. Distilled water was demineralized to a resistance greater than 18 MΩ cm. Horse heart cytochrome *c* (type VI) was purchased from Sigma Chemical Co. The method used to purify chicken SO has recently been described in detail (*10*). Fractions with an $A_{414}/A_{280}$ ratio of >0.93 were pooled together and used for flash photolysis.

*Viscosity.* The absolute viscosities ($\eta$) of water and of aqueous solutions of sucrose were taken from tables (*44*). The relative viscosity ($\eta/\eta_0$) of buffers with and without PEG 400 was measured with a glass viscometer at 293 K; the absolute error was ±0.05 cP. Given that $\eta_0 = 1.002$ cP, the absolute viscosity ($\eta$) was calculated. The contribution of salts to viscosity was neglected. The contribution of proteins to viscosity, since they were present only at micromolar concentrations, was also neglected.

*Laser Flash Photolysis Studies.* 5-Deazariboflavin (dRF), a photoactive species, is excited with a laser pulse, which results in the formation of a semiquinone ($dRFH^{\bullet}$) in the presence of a sacrificial donor such as EDTA or semicarbazide. The semiquinone radical is a strong reducing agent, and rapidly reduces SO to $Fe^{II}Mo^{VI}$. The ensuing slower equilibrium between $Fe^{II}Mo^{VI}$ and $Fe^{III}Mo^{V}$ can subsequently be monitored, by measuring the absorbance change at 555 nm, as shown in Figure 3 (see below). Laser flash photolysis experiments were performed anaerobically on 0.50 mL solutions containing approximately 90 $\mu$M dRF and 0.5 mM semicarbazide as a sacrificial reductant in 10 mM Tris buffer solution (pH 7.4). The concentration of the inhibitory chloride anion was 6.5 mM. The viscosity of the solutions was adjusted by adding an appropriate amount of buffered solutions, at the same pH and ionic strength, of sucrose or PEG 400. Final concentrations of PEG 400 in volume percentage and sucrose in mass percentage are 0−10% and 0−20%, respectively. Buffers with PEG 400 or sucrose were deaerated by vigorous bubbling with argon overnight. Enzyme concentrations were determined by using molar extinction coefficients of 99 900 $M^{-1}$ $cm^{-1}$ at 413 nm for the oxidized chicken SO. The methodology used for flash photolysis has been described previously (*9*). The laser apparatus and associated visible absorbance detection system have been extensively described (*45*), as has the basic photochemical process by which 5-deazariboflavin semiquinone is generated by reaction between triplet-state dRF and the sacrificial reductant semicarbazide and used to reduce redox-active proteins (*46*−*48*). Further details concerning the photochemical process, which are particularly relevant to the SO system, are presented below.

Nonlinear least-squares fitting of transient experimental data obtained at 513 nm was generally performed using an implementation of the Levenberg−Marquart algorithm, provided as part of the Microcal (Northampton, MA) Origin (version 6.1) software package for data processing and display. Transient absorbance changes obtained at 555 nm were analyzed using the computer fitting procedure SIFIT, obtained from OLIS Inc. (Jefferson, GA).

*Steady-State Kinetic Studies.* Steady-state enzyme kinetic studies were performed aerobically in a Varian Cary-300 spectrophotometer, using saturating (10-fold greater than the corresponding $K_m$) concentrations of sulfite (220 $\mu$M), and varying the concentration of cytochrome *c*. Initial velocities were determined by following the reduction of a freshly prepared oxidized cytochrome *c* solution at 550 nm, using an extinction coefficient change of 19 630 $M^{-1}$ $cm^{-1}$ (*49*). Experiments were carried out in 100 mM Tris buffer, adjusted to pH 8.0 with acetic acid to minimize the possibility of anion inhibition.

*EPR Studies.* The *lpH* form was obtained by reduction with excess sodium sulfite in buffers containing 100 mM Tris and 100 mM NaCl (pH 7.0, *lpH*) with or without 20% (w/w) sucrose. CW EPR spectra were recorded at 77 K on an ESP-300E Bruker X-band spectrometer.

## RESULTS AND DISCUSSION

*Steady-State Kinetics of Sulfite Oxidase in the Presence of PEG 400.* The steady-state oxidation of sulfite to sulfate as catalyzed by SO using cytochrome *c* as the electron acceptor yields plots of initial velocity versus substrate concentration that display typical saturation kinetics (Figure 4). The $k_{cat}$ and $K_m^{(cyt\ c)}$ values obtained from these experiments for SO with 0, 10, and 20% (v/v) PEG 400 are listed in Table 1. Within experimental error, these data indicate that PEG 400 has at best a minor effect on the activity (i.e., $k_{cat}$) of SO in the range of viscosity that was studied.

*Effects of Viscosity on Electron Transfer Rates in SO.* Figure 3 shows a typical transient kinetic trace obtained at 555 nm upon laser flash photoexcitation of a solution containing oxidized chicken SO, 5-deazariboflavin, semicarbazide, and 5% (v/v) PEG 400. The transient absorbance

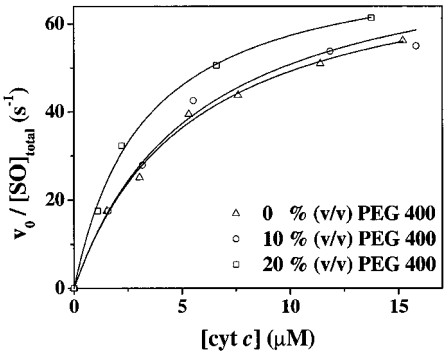


FIGURE 4: Hyperbolic plots of values of initial velocities divided by the total concentration of SO ($1.1 \times 10^{-10}$ M) vs varying concentrations of cyt *c*. Reaction conditions were 0.1 M Tris-acetate buffer at pH 8.0 and 25 °C.

Table 1: $k_{cat}$ and $K_m^{(cyt\ c)}$ Values for Sulfite Oxidase vs Volume Percentage of PEG 400

| PEG % (v/v) | viscosity (cP) | $k_{cat}$ ($s^{-1}$) | $K_m^{(cyt\ c)}$ ($\mu$M) |
|---|---|---|---|
| 0 | 1.002 | $73.2 \pm 3.0$ | $4.3 \pm 0.6$ |
| 10 | 1.653 | $79.6 \pm 5.7$ | $5.4 \pm 0.8$ |
| 20 | 2.735 | $76.0 \pm 2.6$ | $3.3 \pm 0.3$ |

changes observed at this wavelength are directly related to reduction and reoxidation of the *b*-type heme prosthetic group (*7*). As expected, no detectable spectral contribution from the Mo cofactor was observed. It is important to note that SO in the presence of PEG 400 or sucrose has photochemical reduction properties similar to those of SO in the absence of these viscosogens.

The kinetic behavior can be fully described in terms of the minimal set of reactions shown in eqs 2−6 below. Deazariboflavin semiquinone (dRFH$^\bullet$) is generated by the laser pulse in the presence of the sacrificial electron donor semicarbazide ($AH_2$) (eq 3). The initial positive deflection of absorbance from zero in Figure 3 is due to net reduction of the SO heme center to the $Fe^{II}$ form (eq 4), which has an absorbance maximum at 555 nm. The slow decrease in absorbance that follows the initial rapid increase is due to the net IET from $Fe^{II}$ to $Mo^{VI}$, which establishes an equilibrium between the $Mo^{VI}Fe^{II}$ and $Mo^{V}Fe^{III}$ forms of the enzyme (eq 6). The kinetics of this latter process is independent of the concentration of the enzyme within the range of viscosogen concentrations that was used, indicating that it is still due to a first-order intramolecular electron transfer process in the presence of both PEG 400 and sucrose, which is the reaction that is of particular interest to us in this study. The IET rate constant is designated $k_{et}$. If we define $T$ as the total amount of reduced SO present in solution, i.e., $T = [Mo^{VI}Fe^{II}] + [Mo^{V}Fe^{III}]$, and define $X$ as $[Mo^{VI}Fe^{II}]$, according to eq 6, we can write the rate equation for $X$ disappearance as

$$dX/dt = k_r(T - X) - k_f X$$

which readily integrates to (given that $X = T$ at $t = 0$)

$$X = k_r T/k_{et} + k_f T(e^{-k_{et}t})/k_{et}$$

where $k_{et} = k_f + k_r$. Thus, $k_{et}$ is equal to the sum of the forward ($k_f$) and reverse ($k_r$) electron transfer rate constants. This decay curve also provides a means of determining the equilibrium constant $K_{eq}$ ($=k_f/k_r$) for this IET process from the extent of the absorbance decay. To minimize the contribution of AH$^\bullet$ reduction of $Fe^{III}$ (eq 5) and its corresponding spectral overlap with the IET process, semicarbazide was used as a donor in this work instead of EDTA (*9*).

$$dRF \xrightarrow{h\nu} {}^1dRF \rightarrow {}^3dRF \quad (2)$$

$${}^3dRF + AH_2 \rightarrow dRFH^\bullet + AH^\bullet \quad (3)$$

$$dRFH^\bullet + Mo^{VI}Fe^{III} \xrightarrow{k_1} dRF + Mo^{VI}Fe^{II} \quad (4)$$

$$AH^\bullet + Mo^{VI}Fe^{III} \xrightarrow{k_2} AH^+ + Mo^{VI}Fe^{II} \quad (5)$$

$$Mo^{VI}Fe^{II} \underset{k_r}{\overset{k_f}{\rightleftharpoons}} Mo^{V}Fe^{III} \quad (6)$$

The observed rate constant for the initial heme reduction is dependent on protein concentration, as expected for a bimolecular process (eq 4). Electron transfer from dRFH$^\bullet$ to the heme of sulfite oxidase can best be observed spectrophotometrically as a decrease in absorbance at 513 nm, which is close to the absorbance maximum for dRFH$^\bullet$ and an isosbestic point for the oxidized and reduced heme cofactor. Increasing the viscosity by addition of sucrose decreased the second-order rate constant ($k_1$) for electron transfer between heme $b_5$ Fe(III) and the radical dRFH$^\bullet$, from $1.57 \times 10^8$ $M^{-1}$ $s^{-1}$ at 1.0 cP to $1.20 \times 10^8$ $M^{-1}$ $s^{-1}$ at 1.9 cP (data not shown). Increasing the viscosity with PEG 400 had a similar effect. These results are as expected since this heme reduction reaction has a rate constant close to the diffusion-controlled value.

Figure 5A shows that the values of $k_{et}$ decrease progressively with an increase in viscosity. In Figure 5B, normalized values of the IET rate constants are plotted, where $k_{et}^0$ denotes the IET rate constant in the absence of viscosogen. All normalized values, determined in buffered mixtures of water with the two different solutes, PEG 400 and sucrose, fall on the same line when plotted versus the viscosity. It is important to note that recent studies show that the magnetic circular dichroism heme spectra do not change in the presence of PEG 400, suggesting that the heme environment is not affected by this polymer (*50*). Furthermore, the CW EPR spectrum of sulfite-reduced SO in 20% sucrose is the same as that without sucrose (Figure 6), which indicates that the active site structure of the molybdenum domain remains unchanged upon addition of sucrose. In combination with the steady-state kinetic studies described above, we conclude that it is solution viscosity, and not other properties of the added viscosogens and/or their effect on SO structure, that is responsible for the dependence of IET rates on solvent composition.

The viscosity dependence of $k_{et}$ was fitted to the modified Kramers' theory (eq 1) (see Figure 7), which shows that that the IET rate constant in SO has a linear dependence on the negative 0.7th power of the viscosity in the presence of either viscosogen. This dependence can be explained by the following mechanism (see Figure 2)

$$[Mo^{VI}Fe^{II}]_{NR} \underset{k_{-1}}{\overset{k_1}{\rightleftharpoons}} [Mo^{VI}Fe^{II}]_{R} \underset{k_{-2}}{\overset{k_2}{\rightleftharpoons}} [Mo^{V}Fe^{III}]$$

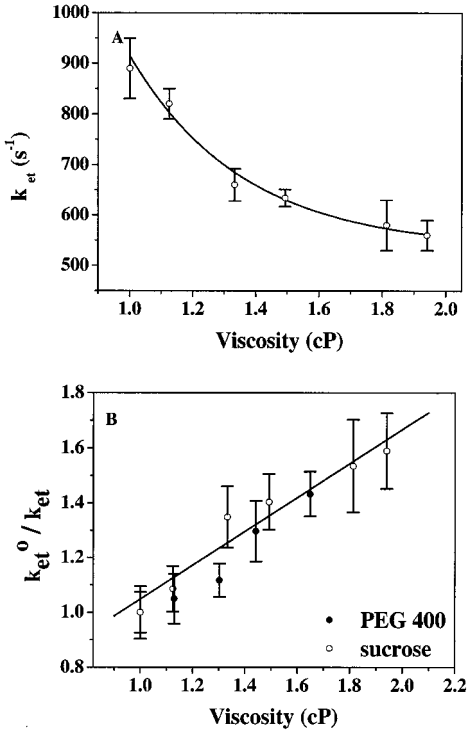


FIGURE 5: (A) Viscosity dependence of the rate constant $k_{et}$ for intramolecular electron transfer in sulfite oxidase, shown in eq 6, in Tris buffer at pH 7.4 using sucrose as a viscosogen. (B) Plot of normalized values ($k_{et}^0/k_{et}$), in which $k_{et}^0$ denotes the rate constant in the absence of viscosogens, vs viscosity, in PEG 400 (●) and sucrose (○). As is evident, the two data sets can be fit by the same line.

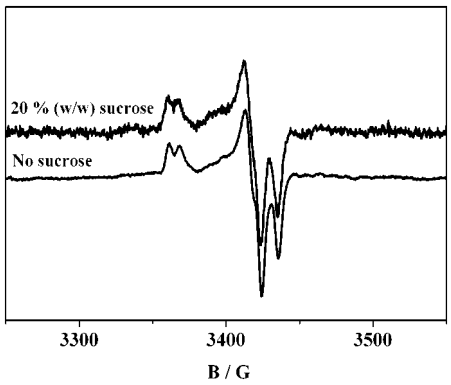


FIGURE 6: Comparison of CW EPR spectra of sulfite-reduced sulfite oxidase in 20% (w/w) sucrose (top spectrum) and no sucrose (bottom spectrum). The buffer is 100 mM Tris, 6.3 mM Tris-HCl, and 100 mM NaCl (pH 7.0).

which shows two conformationally different precursors, being designated NR (for electron transfer nonreactive) and R (for electron transfer reactive). Of the four microscopic rate constants in the above mechanism and in eq 7 derived from it (see below), only $k_1$ and $k_{-1}$ are expected to depend on viscosity with a fractional dependence power

$$k_{et(obsd)} = (k_1k_2 + k_1k_{-2} + k_{-1}k_{-2})/(k_{-1} + k_2 + k_{-2}) \quad (7)$$

giving $1/k_{et(obsd)} \propto \eta^{\alpha}$. Thus, the mechanism is in agreement with the experimental results.

Because the rate constant for electron transfer between the Mo and Fe centers in SO is independent of protein concentration and is thus due to an intramolecular process,

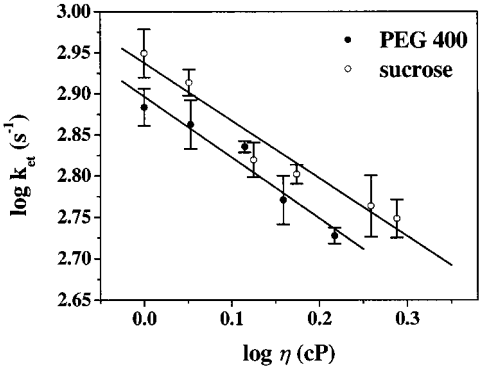


FIGURE 7: Fit of viscosity dependence of the rate constant $k_{et}$ in PEG 400 (●) and sucrose (○) using eq 1.

a plausible explanation for the significant viscosity dependence behavior is that a large conformational change precedes the intramolecular electron transfer in SO. Thus, these results may be considered as indirect evidence that the observed IET rate is not due to the intrinsic electron transfer process, but rather is gated by a protein conformational change, presumably mediated by the domain-connecting loop in SO. Further experiments in which this loop is shortened by site-directed mutagenesis are underway and will provide more direct evidence for the role of the flexibility of this portion of the molecule in electron transfer in SO.

## ACKNOWLEDGMENT

We thank Drs. Andrew Pacheco and Rachel Codd for their informative discussions. We thank Dr. Arnold M. Raitsimring for determination of the EPR spectra.

## REFERENCES

1. Hille, R. (1996) *Chem. Rev. 96*, 2747−2816.
2. Cohen, H. J., Betcher-Lange, S., Kessler, D. L., and Rajagopalan, K. V. (1972) *J. Biol. Chem. 247*, 7759−7766.
3. Kessler, D. L., Johnson, J. L., Cohen, H. J., and Rajagopalan, K. V. (1974) *Biochim. Biophys. Acta 334*, 86−96.
4. Garrett, R. M., Bellissimo, D. B., and Rajagopalan, K. V. (1995) *Biochim. Biophys. Acta 1262*, 147−149.
5. Garrett, R. M., and Rajagopalan, K. V. (1994) *J. Biol. Chem. 269*, 272−276.
6. Neame, P., and Barber, M. J. (1989) *J. Biol. Chem. 264*, 20894−20901.
7. Sullivan, E. P., Jr., Hazzard, J. T., Tollin, G., and Enemark, J. H. (1993) *Biochemistry 32*, 12465−12470.
8. Schindelin, H., Kisker, C., and Rajagopalan, K. V. (2001) in *Advances in Protein Chemistry*, Vol. 58, pp 47−94, Academic Press, San Diego.
9. Pacheco, A., Hazzard, J. T., Tollin, G., and Enemark, J. H. (1999) *J. Biol. Inorg. Chem. 4*, 390−401.
10. Kisker, C., Schindelin, H., Pacheco, A., Wehbi, W., Garrett, R. M., Rajagopalan, K. V., Enemark, J. H., and Rees, D. C. (1997) *Cell 91*, 973−983.
11. Gray, H. B., and Winkler, J. R. (1996) *Annu. Rev. Biochem. 65*, 537−561.
12. Page, C. C., Moser, C. C., Chen, X., and Dutton, P. L. (1999) *Nature 402*, 47−52.
13. Frauenfelder, H., Wolynes, P. G., and Austin, R. H. (1999) *Rev. Mod. Phys. 71*, S419−S430.
14. Falke, J. J. (2002) *Science 295*, 1480−1481.
15. Kramers, H. A. (1940) *Physica (Amsterdam) 7*, 284−304.
16. Rosskey, P. J., and Simon, J. D. (1994) *Nature 370*, 263−269.
17. Sumi, H. (2001) *J. Mol. Liq. 90*, 185−194.
18. Gavish, B. (1978) *Biophys. Struct. Mech. 4*, 37−52.

19. Gavish, B., and Werber, M. M. (1979) *Biochemistry 18*, 1269−1275.
20. Gavish, B., and Yedgar, S. (1994) in *Protein−Solvent Interactions* (Gregory, R. B., Ed.) pp 343−373, Marcel Dekker, New York.
21. Gutfreund, H. (1995) in *Kinetics for the Life Science: Receptor, Transmitters and Catalysts*, Chapter 7, pp 231−280, Cambridge University Press, New York.
22. Beece, D., Eisenstein, H., Frauenfelder, H., Good, D., and Marden, M. C. (1980) *Biochemistry 19*, 5147.
23. Schlitter, J. (1988) *Chem. Phys. 120*, 187−197.
24. Bhattacharyya, R. P., and Sosnick, T. R. (1999) *Biochemistry 38*, 2601−2609.
25. Wallace, M. I., Ying, L. M., Balasubramanian, S., and Klenerman, D. (2001) *Proc. Natl. Acad. Sci. U.S.A. 98*, 5584−5589.
26. Martin, S. F., and Hergenrother, P. J. (1999) *Biochemistry 38*, 7265−7272.
27. Skamnaki, V. T., Owen, D. J., Nobel, M. E. M., Lowe, E. D., Lowe, G., Oikonomakos, N. G., and Johnson, L. N. (1999) *Biochemistry 38*, 14718−14730.
28. Chen, G., Porter, M. D., Bristol, J. R., Fitzgibbon, M. J., and Pazhanisamy, S. (2000) *Biochemistry 39*, 2079−2087.
29. Kawai, Y., Matsuo, T., and Ohno, A. (2000) *J. Chem. Soc., Perkin Trans. 2*, 887−897.
30. Goldbeck, R. A., Paquette, S. J., and Kliger, D. S. (2001) *Biophys. J. 81*, 2919−2934.
31. Hagen, S. J., Hofrichter, J., and Eaton, W. A. (1995) *Science 269*, 959−962.
32. Ansari, A., Jones, C. M., Henry, E. R., Hofrichter, J., and Eaton, W. A. (1992) *Science 256*, 1796−1798.
33. Walser, R., and van Gunsteren, W. F. (2001) *Proteins: Struct., Funct., Genet. 42*, 414−421.
34. Fayer, M. D. (2001) *Annu. Rev. Phys. Chem. 52*, 315−356.
35. Jas, G. S., Eaton, W. A., and Hofrichter, J. (2001) *J. Phys. Chem. B 105*, 261−272.
36. Davidson, V. L. (1996) *Biochemistry 35*, 14035−14039.
37. Hoffman, B. M., and Ratner, M. A. (1987) *J. Am. Chem. Soc. 109*, 6237−6243.
38. Ivkovic-Jensen, M. M., Ullmann, G. M., Young, S., Hansson, O., Crnogorac, M. M., Ejdeback, M., and Kostic, N. M. (1998) *Biochemistry 37*, 9557−9569.
39. Pletneva, E. V., Fulton, D. B., Kohzuma, T., and Kostic, N. M. (2000) *J. Am. Chem. Soc. 122*, 1034−1046.
40. Ivkovic-Jensen, M. M., Ullmann, G. M., Crnogorac, M. M., Ejdeback, M., Young, S., Hansson, O., and Kostic, N. M. (1999) *Biochemistry 38*, 1589−1597.
41. Mei, H. K., Wang, K. F., Peffer, N., Weatherly, G., Cohen, D. S., Miller, M., Pielak, G., Durham, B., and Millett, F. (1999) *Biochemistry 38*, 6846−6854.
42. Harris, M. R., Davis, D. J., Durham, B., and Millett, F. (1997) *Biochim. Biophys. Acta 1319*, 147−154.
43. Heimann, S., Ponamarev, M. V., and Cramer, W. A. (2000) *Biochemistry 39*, 2692−2699.
44. *CRC Handbook of Chemistry and Physics*, 66th ed. (1986) (Weast, R. C., Ed.) CRC Press, Boca Raton, FL.
45. Hurley, J. K., Weber-Main, A. M., Stankovich, M. T., Benning, M. M., Thoden, J. B., Vanhooke, J. L., Holden, H. M., Chae, Y. K., Xia, B., Cheng, H., Markley, J. L., Martinez-Julvez, M., Gomez-Moreno, C., Schmetis, J. L., and Tollin, G. (1997) *Biochemistry 36*, 11100−11117.
46. Tollin, G., Hurley, J. K., Hazzard, J. T., and Meyer, T. E. (1993) *Biophys. Chem. 48*, 259−279.
47. Tollin, G. (1995) *J. Bioenerg. Biomembr. 27*, 303−309.
48. Tollin, G. (2001) in *Electron Transfer in Chemistry* (Balzani, V., Ed.) Vol. IV, pp 202−231, Wiley-VCH, Weinheim, Germany.
49. Brody, M. S., and Hille, R. (1999) *Biochemistry 38*, 6668−6677.
50. Helton, M. E., Pacheco, A., McMaster, J., Enemark, J. H., and Kirk, M. L. (2000) *J. Inorg. Biochem. 80*, 227−233.

BI016059F